Biophysical Chemistry 137 (2008) 13–18

Contents lists available at ScienceDirect

Biophysical Chemistry

journal homepage: http://www.elsevier.com/locate/biophyschem

# Effect of a single point mutation on the stability, residual structure and dynamics in the denatured state of GED: Relevance to self-assembly

Jeetender Chugh [a,1], Shilpy Sharma [a,1], Dinesh Kumar [a], Jyoti R. Misra [b], Ramakrishna V. Hosur [a,*]

[a] Department of Chemical Sciences, Tata Institute of Fundamental Research, Homi Bhabha Road, Mumbai-400005, India
[b] Department of Biological Sciences, Tata Institute of Fundamental Research, Homi Bhabha Road, Mumbai-400005, India

ARTICLE INFO

*Article history:*
Received 15 May 2008
Received in revised form 5 June 2008
Accepted 5 June 2008
Available online 17 June 2008

*Keywords:*
Circular dichroism
Denatured state
Fluorescence spectroscopy
GTPase effector domain
Nuclear magnetic resonance

ABSTRACT

The GTPase effector domain (GED) of dynamin forms large soluble oligomers *in vitro*, while its mutant – I697A – lacks this property at low concentrations. With a view to understand the intrinsic structural characteristics of the polypeptide chain, the global unfolding characteristics of GED wild type (WT) and I697A were compared using biophysical techniques. Quantitative analysis of the CD and fluorescence denaturation profiles revealed that unfolding occurred by a two-state process and the mutant was less stable than the WT. Even in the denatured state, the mutation caused chemical shift perturbations and significant differences were observed in the $^{15}N$ transverse relaxation rates ($R_2$), not only at the mutation site but all around. These results demonstrate that the hydrophobic change associated with the mutation perturbs the structural and motional preferences locally, which are then relayed via different folding pathways along the chain and the property of oligomerization in the native state is affected.



## 1. Introduction

Equilibrium (un)folding studies have been used to gain insights about the native states of proteins in terms of their intrinsic stability, cooperativity and the structural changes that occur as these (un)fold [1,2]. Various biophysical as well as computational means have been devised to investigate the (un)folding pathways of proteins [3–6], the energy landscape of which have been described in terms of a folding funnel [7]. The broad end of this funnel reflects the heterogeneous 'unfolded' or unstable states of the protein where the protein is no longer functionally active (except for intrinsically denatured proteins which are active in that state) and are more prone to aggregation as a consequence of misfolding, while the narrow end of the funnel reflects the fully 'folded' or the native state of the protein [7–9]. Amongst the biophysical techniques used, circular dichroism (CD) and steady-state fluorescence have been widely used to understand the global characteristics, while residue-level insights have been obtained using multi-dimensional NMR at different denaturation conditions [10–13].

Dynamin, an important multi-domain protein, plays a key role in the endocytosis process [14–16]. Its GTPase effector domain (GED) plays an important role in both dynamin function and assembly [16]. The biophysical characterization of GED has shown that it forms large soluble oligomers in native conditions *in vitro* [17]. Mutational analysis of GED from isoleucine (I) at the position 697 to lysine (K) suggested that interaction with an amphipathic helix in GED is required for dynamin self-assembly [16]. In addition to this, the I697 site in human dynamin corresponds to L612 in human MxA protein, which has characteristics similar to dynamin *in vitro*; it can self-assemble, has assembly-stimulated GTPase activity and can tubulate liposomes [18,19]. Mutations at both I697 in dynamin [16] and L612 in MxA [20] have been known to abrogate the self-assembly process. Furthermore, since hydrophobic collapse is an important cause of oligomerization, mutations that alter the hydrophobicity could play an important role in this process. Thus, in order to investigate the effect of hydrophobicity on protein structure and its property of forming oligomers, mutation at I697 to alanine (neutral residue with a smaller side chain) was performed [17]. The substitution of isoleucine with alanine not only reduces the length and hydrophobic volume of the side chain, but also changes the conformational propensity along the chain; alanine is known to induce flexibility in the polypeptide chain and act as molecular hinge [21]. Interestingly, this site lies in the residues identified for initiation of GED self-assembly [22]. Interestingly, this mutation inhibited the self-association of protein quite significantly at lower concentrations *in vitro* [17].

Just as the characteristics of the final folded state of a protein are largely dictated by the amino acid sequence, though the environment has a certain role to play, the association characteristics would also be intrinsic to the protein. These intrinsic characteristics can be best investigated under conditions, where the protein remains largely unfolded. Earlier NMR-based studies on guanidine-denatured wild

* Corresponding author. Department of Chemical Sciences, Tata Institute of Fundamental Research, 1, Homi Bhabha Road, Mumbai-400005, India. Tel.: +91 22 22782271, +91 22 22782488; fax: +91 22 22804610.
*E-mail address:* hosur@tifr.res.in (R.V. Hosur).
[1] Both authors contributed equally.

0301-4622/$ – see front matter © 2008 Elsevier B.V. All rights reserved.
doi:10.1016/j.bpc.2008.06.005

type (WT) GED showed the presence of four clusters of residues that displayed differential dynamics [23] along the polypeptide chain. These clusters could be identified as initiation sites for folding and association when suitable conditions are provided. It is therefore likely that inter- and intra-molecular interaction between these clusters might be responsible for GED association and hence dynamin oligomerization during endocytosis. With this background, we present here the biophysical studies on the unfolding of GED WT and I697A in the presence of Guanidine–HCl (Gdn–HCl). The global unfolding characteristics, studied using optical techniques and the residue-level dynamics of the unfolded states, as obtained from the relaxation analysis using multi-dimensional NMR, have been compared for GED and its mutant, I697A.

## 2. Experimental

### 2.1. Protein expression and purification

GED WT and I697A were expressed and purified as described earlier [23]. As discussed earlier [23], the 618th residue of dynamin corresponds to the third residue in the recombinant GED clones and the amino acids in all discussions and figures have been numbered accordingly. The site of mutation Ile697 in dynamin is actually Ile82 in recombinant GED.

### 2.2. Circular dichroism

Far-UV CD spectra were recorded at 27 °C on a JASCO J-810 spectropolarimeter (Jasco, Europe) using 1 nm band-width. All experiments were recorded using 20 μM protein in a fused quartz cell with a path length of 1 mm. Scans were acquired from 210 to 260 nm with a scan speed of 50 nm/min. Each spectrum was an average of 5 scans. The protein samples were equilibrated, with different concentrations of Gdn–HCl, at least 12 h before recording the experiment and the denaturation profiles were measured at intervals of 0.2 M in the range of 0–6 M Gdn–HCl. At the end of these experiments, the CD spectra were re-recorded for a few concentrations. These spectra were found to be unaltered, thereby indicating that the samples had acquired equilibrium before acquisition. All the measurements were repeated thrice with freshly prepared samples on different days to check for the reproducibility of the profiles. All spectra were base line corrected by recording the blanks with different concentrations of the denaturant and subtracting these values from those of the protein recorded under identical conditions. The data, thus obtained, were smoothened by three-point averaging to minimize errors due to denaturant concentration adjustments and then normalized using the following equation [13]:

$$F_{app} = \frac{S_{obs} - S_F}{S_U - S_F} \tag{1}$$

where, $F_{app}$ is the relative CD value depicting the apparent unfolded fraction, $S_{obs}$ is the observed CD signal in the presence of the denaturant. $S_F$ and $S_U$, in turn, are defined by the following equations:

$$S_F = k_F[D] + b_F$$

and

$$S_U = k_U[D] + b_U$$

where, $k_F$; $k_U$ and $b_F$; $b_U$ define the slopes and constants for the pre- and post-transition baselines and $[D]$ is the denaturant concentration.

### 2.3. Fluorescence measurements

Bis-ANS (Molecular Probes, OR, USA) was prepared and the concentration was determined using the extinction coefficient, $\varepsilon_{360}$=23,000 $cm^{-1}$ $M^{-1}$. Steady-state fluorescence emission spectra were recorded with $\lambda_{exc}$=395 nm on a Spex FLuorolog-dM3000F spectrofluorimeter at 27 °C using a 1 cm path length cuvette with a band pass of 1.5 nm for both excitation and emission. The emission spectra were measured from 450 to 550 nm at a scan rate of 1 nm $s^{-1}$. The denaturation profiles of 10 μM protein in tris buffer (20 mM, pH 7.4), pre-equilibrated with varying concentration of the denaturant and bis-ANS (4 μM) for 12 h were measured, by monitoring the emission at 491 nm. The data were smoothened by three-point averaging to minimize errors due to denaturant concentration adjustments and were normalized using the following equation [13]:

$$F_{app} = \frac{S_F - S_{obs}}{S_F - S_U} \tag{2}$$

where, the definitions for the individual entities remain the same.

### 2.4. Data analysis

The data for the unfolding transitions probed by CD (a secondary structure probe) and fluorescence (a tertiary structure probe) were quantitatively analyzed according to two-state (N⇔U) and three-state transition models (N⇔I⇔U), depending upon the best fit obtained. The following Eqs. (3) and (4), obtained from the equation for fitting multi-state transition derived from the law of mass action concept [24,25], were used to fit the data to two-state transition and three-state transitions, respectively.

$$A_{obs} = \frac{A_0 + A_{11}\exp-\frac{(\Delta G_1^0 - m_1[D])}{RT}}{1 + \exp-\frac{(\Delta G_1^0 - m_1[D])}{RT}} \tag{3}$$

$$\text{and, } A_{obs} = \frac{A_0 + A_{11}\exp-\frac{(\Delta G_1^0 - m_1[D])}{RT} + A_u\exp-\frac{(\Delta G_1^0 + \Delta G_2^0 - (m_1+m_2)[D])}{RT}}{1 + \exp-\frac{(\Delta G_1^0 - m_1[D])}{RT} + \exp-\frac{(\Delta G_1^0 + \Delta_2^0 - (m_1+m_2)[D])}{RT}} \tag{4}$$

where, $\Delta G^0$ is the free energy change at every step; $m_i$ indicates the dependence of free energy on the denaturant concentration $[D]$ and $A$s are the specific contributions of each species to the signals. $R$ and $T$ are the gas constant and absolute temperature, respectively. The molarity values for the transition mid-points ($C_m$ values) have been reproduced from the simulations used for the two-state fit model, and the reported mid-points correspond to the value of the denaturant at which $F_{app}$ equals 0.50.

### 2.5. NMR spectroscopy

#### 2.5.1. NMR sample

For NMR-based studies, isotopically rich protein samples ($^{15}N$) were prepared using M9 media containing $^{15}NH_4Cl$ as the sole source of nitrogen, described earlier [23], and concentrated to a concentration of 1 mM. The sample was exchanged with acetate buffer (10 mM acetate, pH 5.0) containing 1 mM EDTA, 150 mM NaCl, 1 mM DTT and 6 M Gdn–HCl. The samples were allowed to attain equilibrium before the start of the experiment.

#### 2.5.2. NMR data acquisition and processing

All the NMR experiments were recorded on a Bruker Avance spectrometer equipped with CryoProbe and triple resonance probes, operating at $^1H$ frequency of 800 MHz. The $^1H$ and $^{15}N$ carrier frequencies were set at 4.69 (water) and 118 ppm, respectively. HSQC experiments were recorded at the start and at the end of the experiments and compared to check the stability of the proteins. No change was observed in these HSQC spectra indicating that the protein was highly stable under the experimental conditions and had attained equilibrium at the beginning of the experiment. All experiments were

processed and analyzed using Felix (Accelrys Software Inc., San Diego, CA, USA). All relaxation experiments were carried out using the pulse sequences as described earlier [26]. $^{15}N$ transverse relaxation rates ($R_2$) were measured using CPMG delays of 10, 30, 50*, 90, 130, 170*, 230 and 300 ms, where asterisks indicate points recorded in duplicate for standard error calculations.

In all the NMR experiments, $^{1}H$ chemical shifts were referenced to HDO [4.598 ppm with respect to 2, 2-dimethyl-2-silapentane-5-sulphonic acid (DSS) at 15 °C, 6 M Gdn–HCl in acetate buffer, pH 5.0] while the $^{13}C$ and $^{15}N$ chemical shifts were indirectly referenced to DSS.

## 3. Results and discussion

### *3.1. Gdn–HCl-mediated denaturation profile of GED isoforms by circular dichroism and fluorescence*

The unfolding of small compact proteins has been interpreted by a simple two-state cooperative transition, wherein the probability of finding the intermediates between the native and the unfolded/denatured states is low [27,28]. In such a case, the unfolding transitions measured by different probes are found to be identical. However, intermediate states different from native or completely unfolded state have been recognized in the unfolding/folding steps of several proteins including bovine and human isoforms of carbonic anhydrase β, β-lactamase, bovine growth hormones, etc [29]. The data for such transitions are analyzed using three-, four- or multi-state models [30–32]. The characterization of these folding intermediates further help in the identification of various transition steps and the conformational changes that occur in the protein on interaction with different denaturants and thus provide insight into the folding process of the protein.

The unfolding of GED WT and I697A proteins by Gdn–HCl was found to be reversible. The CD and fluorescence spectra of freshly prepared protein and the refolded one from 6 M Gdn–HCl condition were found to be identical. The Gdn–HCl concentrations were varied from 0 M to 6 M, with each sample differing by 0.2 M. The changes in molar ellipticity in far-UV CD reflect the changes in the secondary structure of a protein while the changes in fluorescence emission reflect the changes in its tertiary structure. For a protein which follows cooperative two-state transitions, the denaturation profiles obtained by both the spectroscopic parameters overlap and have typical sigmoidal shapes.

The normalized denaturation profiles for the GED WT and I697A, obtained by monitoring ellipticity at 222 nm in far-UV CD spectroscopy (normalized using Eq. (1)) and by monitoring the fluorescence property of the protein-bis-ANS complex at an emission maximum of 491 nm (normalized using Eq. (2)), are shown in Fig. 1a and b, respectively. In case of a protein like GED, known to form a large self-assembly [22], the denaturation process may first involve the dissociation of the oligomer and then the monomers would unfold. Thus the process could be quite complex and if the dissociated monomers are unstable, the two-state model would provide the best fits. We tried to analyze these data according to two-state and three-state models as per Eqs. (3) and (4), respectively. In every case, the two-state model ($N \Leftrightarrow U$) gave the best fits; the three-state model gave large fitting errors (data not shown). The thermodynamic parameters thus derived have been summarized in Table 1.

Even though the two-state model gave the best fits to the denaturation profiles, the global unfolding does not seem to be cooperative in case of GED WT as the curve obtained by CD (which senses the overall secondary structural changes) does not exactly superimpose over the unfolding trace obtained by fluorescence (Fig. 1a). Although, the fluorescence and the CD curves converge in the initial and the final unfolding steps, differences are observed in the two profiles between 2 M and 5 M Gdn–HCl. This would mean that the unfolding proceeds via an intermediate, which, however, is very unstable to be explicitly detected. Nonetheless, the two spectra yield very close transition mid-points (2.52 M from steady-state fluorescence and 2.77 M from far-UV CD). A small hump, within the range of baseline fluctuations, was also observed in the fluorescence spectra of the WT (~0.75 M Gdn–HCl).

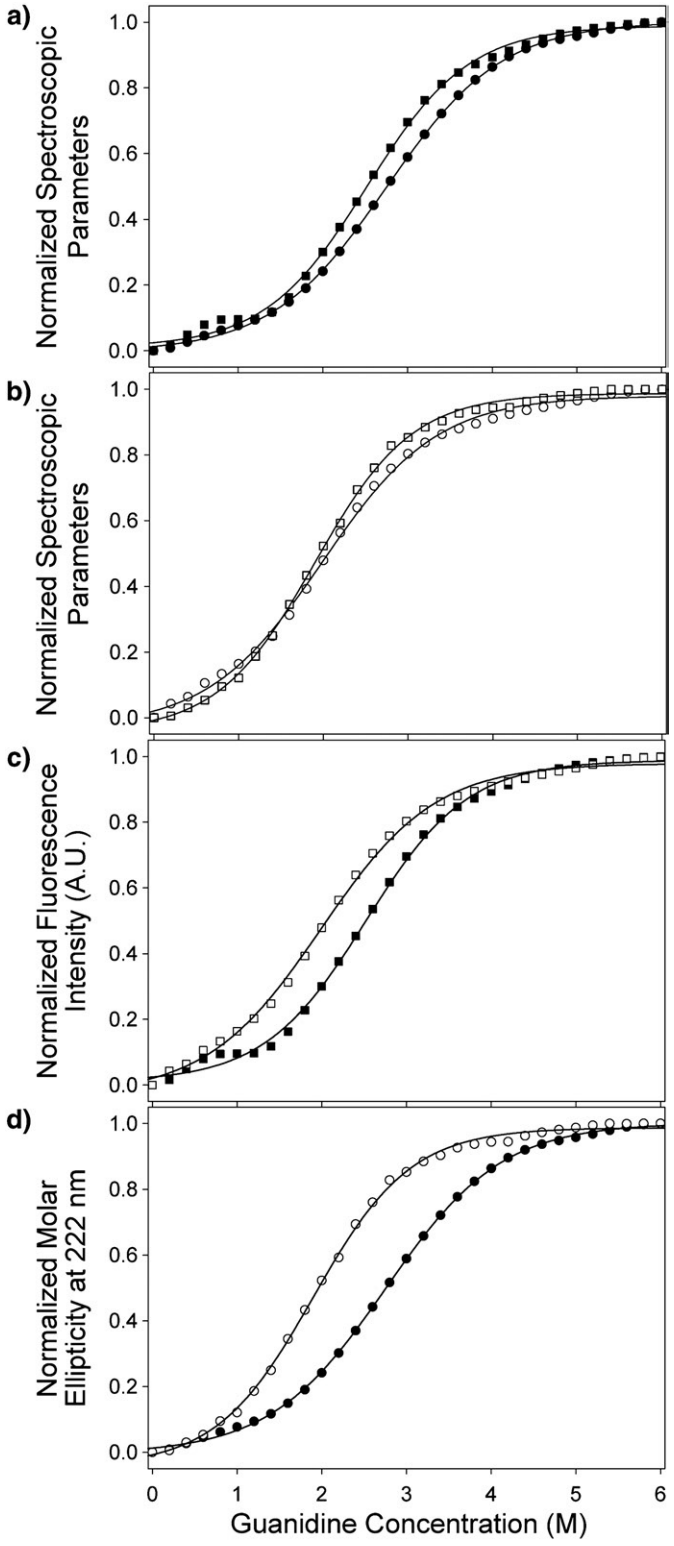


**Fig. 1.** Normalized spectroscopic parameters [CD (circles) and steady-state fluorescence (squares)] for the Gdn–HCl mediated denaturation of a) GED WT (filled symbols) and b) I697A (empty symbols). Comparison of the normalized c) fluorescence and d) CD spectra for the WT and I697A proteins. The solid lines represent the best fits obtained using the 2-state model (see text).

**Table 1**
The thermodynamic parameters derived from fits to the two-state model (N↔U) for Gdn–HCl mediated denaturation for GED WT and I697A in TEND buffer, pH 7.4

| | | $\Delta G$ (kJ mol$^{-1}$) | $m$ (kJ mol$^{-1}$ M$^{-1}$) | $C_m$ (M) |
|---|---|---|---|---|
| WT | CD | 10.45±0.37 | 3.64±0.05 | 2.77 |
| | Fluorescence | 10.05±0.00 | 4.14±0.15 | 2.52 |
| I697A | CD | 8.23±0.25 | 4.34±0.12 | 1.97 |
| | Fluorescence | 7.33±0.35 | 3.69±0.15 | 2.07 |

The I697A protein, on the other hand displays somewhat different unfolding characteristics (Fig. 1b). The CD and the fluorescence profiles were found to be largely super-imposable except between 0–1 M and 2–4 M Gdn–HCl. The transition mid-point for the tertiary structure opening is 1.97 M and is very close to the transition mid-point for the opening of the secondary structure (2.07 M). These suggest a greater degree of cooperativity in the global unfolding of I697A protein.

When the fluorescence intensities were compared for the GED WT and the mutant proteins (Fig. 1c), it was observed that the tertiary structure unfolds earlier, and to a greater extent, in I697A when compared to the WT. The transition mid-points for WT and I697A were 2.52 M and 2.07 M, respectively and were significantly different from each other. Consistent with these findings, when the secondary structure unfolding for GED WT and I697A, as monitored by CD, were compared (Fig. 1d), it was observed that the mutant protein starts unfolding earlier than the WT. The transition mid-points in this case were 2.77 M and 1.97 M for the WT and I697A, respectively, which are significantly different from each other. Also, the secondary structure in case of I697A unfolds almost completely at a Gdn–HCl concentration of ~3.2 M while ~4.2 M Gdn–HCl is required to attain the same amount of denaturation (90%) in the WT. Moreover, as expected, the free energy changes are not the same. The WT is associated with higher free energy as compared to I697A (Table 1); the observed difference must be attributed to the different free energies of the folded and the unfolded states of the two. Thus, it can be concluded that both the tertiary and the secondary structures of the I697A protein are thermodynamically less stable when compared to those of the WT.

### 3.2. Chemical shift perturbations

Next, to see the intrinsic structural preferences of the GED WT and I697A proteins, we monitored the $^{1}$H and $^{15}$N chemical shifts in their 6 M Gdn–HCl denatured states. Fig. 2a shows an overlay of the $^{1}H^{N}$-$^{15}N$ HSQC spectra of the two proteins. It is seen that the spectra superimpose in many places, but there are also small differences for many peaks. While, the close similarity of the spectra permits transfer of assignments from one to the other (rare ambiguities due to closeness of peaks were resolved from spin system identification from TOCSY-HSQC spectra), the small differences reflect upon the intrinsic structural differences. The residue-wise summed chemical shift changes ($\Delta\delta$) were calculated using the following Eq. (5):

$$\Delta\delta\left[(\Delta H)^2+\left(\frac{\Delta N}{10}\right)^2\right]^{\frac{1}{2}} \tag{5}$$

where, $\Delta H$ and $\Delta N$ signify the changes in the amide and $^{15}$N chemical shifts, respectively. The factor of 10 for the $^{15}$N chemical shift arises as a normalization factor since the overall range of nitrogen chemical shifts is roughly 10 times that of the proton chemical shifts for the backbone amides. The results of these chemical shift perturbations have been depicted in Fig. 2b. Clearly, the I697A mutation causes

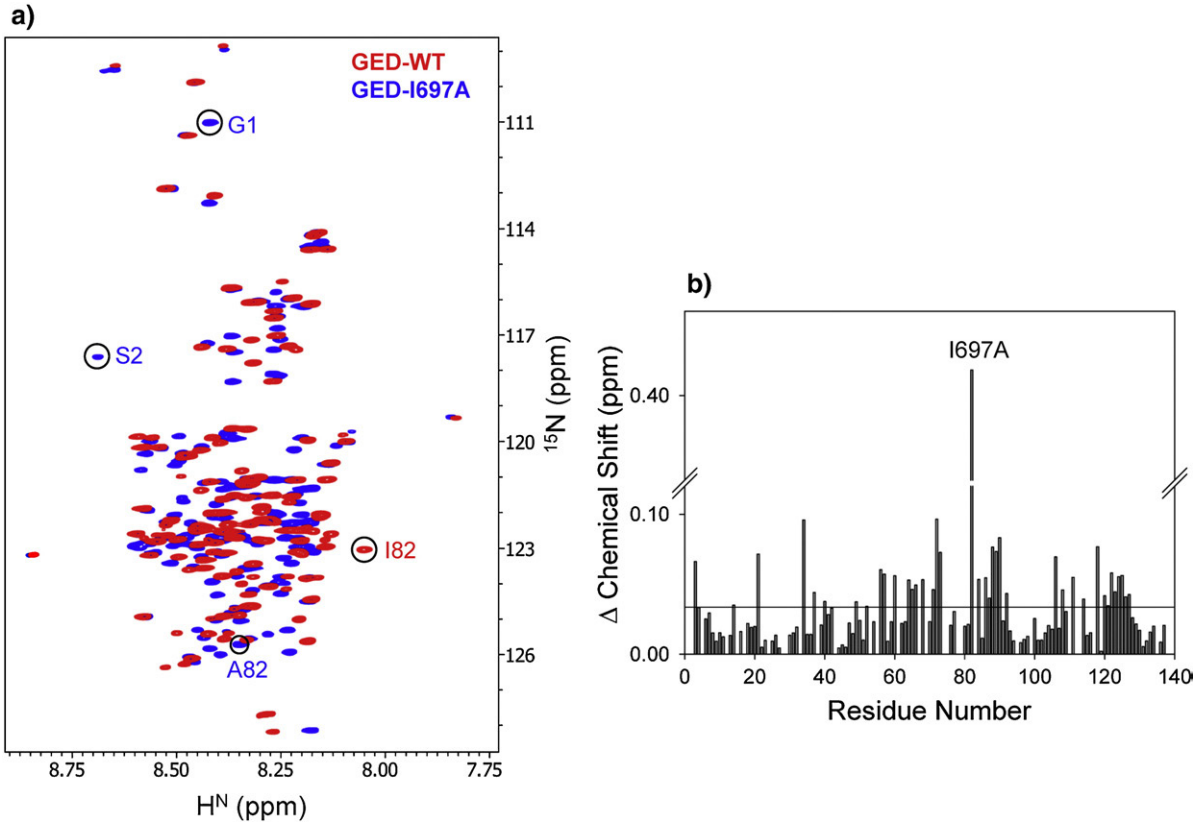


**Fig. 2.** a) Overlay of the $^{1}H^{N}$-$^{15}N$ HSQC spectra of the GED wild type [WT (red)] and I697A (blue) at pH 5.0 and 15 °C. The peaks corresponding to Ile82 in the WT and Ala82 in the I697A mutant have been encircled and annotated by their respective color codes. The peaks for Gly1 and Ser2, visible in the I697A spectrum, have been marked; b) Residue-wise summed chemical shift changes ($\Delta\delta$) between the WT and the I697A mutant of GED calculated from $\Delta H^N$ and $\Delta N$ shifts (see text).

significant perturbations along the sequence not only at the site of the mutation (i.e., Ile82 in the numbering scheme used) but all around. As can be seen, residues Ala3, Ala21, His34, Ala56, Ile57, Lys60, Asp64, Met71–Leu73, Ala88–Leu90, Gln106, Arg109, His118, Ile127 show distinct differences. Our earlier work on the characterization of the 6 M Gdn–HCl denatured GED identified four clusters of residues (marked as A, B, C and D) with significant non-random structures [23]. Of these, B, C and D largely belong to those regions where secondary structures (mostly α-helical) were predicted in the native state [17]. The mutation, I697A at residue 82, lies in the identified cluster C. It is, however, observed now that the mutation resulted in perturbations in the chemical shifts not only in the residues from cluster C (Ala88–Leu90), but also in residues from the clusters A (Ala21), B (His34, Ala56, Ile57, Lys60), D (Gln106, Arg109, His118), in residues between the clusters B and C (Met71–Leu73) and in the N- and the C-terminals (Ala3, Ile127). Thus, the perturbations in the residual structure due to the single point mutation seem to get relayed all across the chain.

### 3.3. Conformational dynamics

$^{15}$N transverse relaxation rates ($R_2$) in a protein are largely sensitive to slow motions and reflect contributions from slower exchange processes that occur in the milli-second to micro-second time scales. For instance, an increase in the conformational exchange leads to a prominent increase in these rates. In case of denatured proteins, these have been used to gain valuable insights into the sequence-dependent motional restrictions and flexibilities [33]. Thus, in order to investigate the effect of the I697A mutation on the conformational dynamics, the transverse relaxation rates were measured for the mutant in 6 M Gdn–HCl and were compared with those of the WT reported earlier [23]. Fig. 3a and b depicts the $R_2$ values for GED WT and I697A, respectively for all the residues (106 in number) for which the data are available for both the proteins.

The $R_2$ relaxation rate in GED WT showed considerable variation ranging from 2.54±0.01 $s^{-1}$ to 8.99±0.02 $s^{-1}$ (average being 5.88±0.21 $s^{-1}$), and four different clusters of residues, A, B, C and D displaying distinct motional characteristics were identified [23]. These were associated with significant non-random structures. The $R_2$ values were lower for the N- and the C-terminal residues indicating increased flexibility in these regions of the protein.

The $R_2$ relaxation rates in the I697A mutant protein (Fig. 3b) also displayed sequence-specific variations ranging from 3.88±0.10 $s^{-1}$ to 9.51±0.43 $s^{-1}$, similar to those in the WT protein and the average $R_2$ value (5.56±0.24 $s^{-1}$) was also similar to that for the WT. However, the minimum and the maximum $R_2$ values showed considerable difference (Fig. 3b).

The differences in the residue-wise $R_2$ values between the WT and I697A have been depicted in Fig. 3c. Interestingly, substantial differences are observable. The positive and the negative deviations indicate decrease or increase in $R_2$, respectively with respect to the WT, and represent decreased and increased conformational exchange in the unfolded state of the mutant. These deviations roughly belong to three major categories: large (> ±1.5 $s^{-1}$), intermediate (±1.5 to 0.5 $s^{-1}$) and small (< ±0.5 $s^{-1}$). Of these, the third class cannot be considered significant as the values are roughly similar to the errors in the measurement. As can be seen from Fig. 3c, large positive deviations (> −2.5 $s^{-1}$) are observed for $R_2$ values at residues Phe81 and Ala82, which correspond to the site of the mutation. This signifies decrease in $R_2$ values in the mutant when compared to the wild type which may be attributed to flexibility induced by the alanine residue in the mutant [21]. Similar large positive deviations (> −1.5 $s^{-1}$) are also observed for the residues His34, Ile57, Lys60 and Met116. It is important to note here that His34, ILe57 and Lys60 belong to the cluster B (predicted helix 1) while Met116 belongs to the cluster D (predicted helix 2). On the other hand, large negative deviations (> +1.5 $s^{-1}$) are observed for the N-terminal Ala3; Val10 and Ala21 from cluster A; Met71–Leu73 from the region between cluster B and C; Leu86 from cluster C; and His118 from cluster D (predicted helix 2). As discussed in the previous section, several of these residues including Ala3, Ala21, His34, Ile57, Lys60, Met71–Leu73 and His118 displayed changes in the chemical shifts in the mutant when compared to the WT (Fig. 2b). The increase in the $R_2$ values for those residues widely spread out along the sequence may be attributed to transient folding and interactions between those residues, which, in turn, could argue for the structural perturbations at those sites as evidenced by chemical shift perturbations.

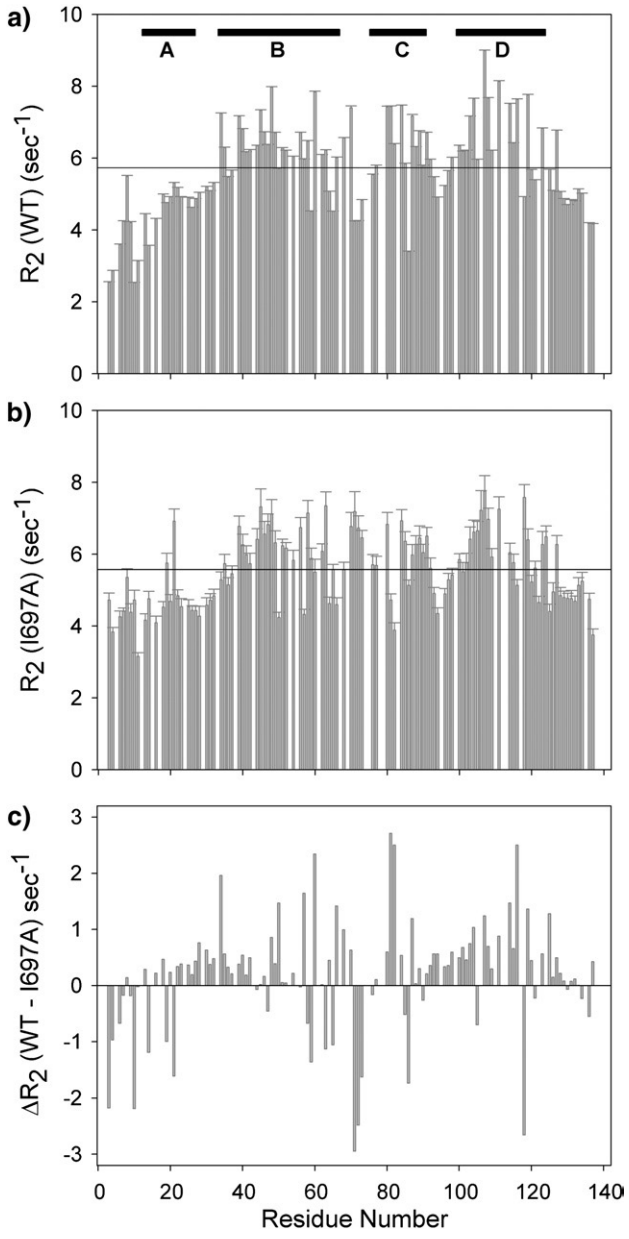


**Fig. 3.** Residue-wise $^{15}$N transverse relaxation rates ($R_2$) for a) GED WT; b) I697A and c) difference of $R_2$s (WT − I697A) in 10 mM Acetate buffer at pH 5.0 and 15 °C. The black bars [marked as A (Glu 13–Glu 26), B (His34–Met 66), C (Asn 76–Leu 90), and D (Met 100–Ala 123)] at the top represent areas of significant non-random structures [23].

Additionally, intermediate positive deviations were also observed for the residues Asp30, Ser35, Leu40, Arg48, Lys50 and Met66 from the cluster B; Lys68 between B and C; residues Glu80, Ser84, Leu87 from the cluster C; residues Glu101–Ala104, Ala107, Gln108, Asp111, Leu114–Arg115, Ala119 and Ala123 from cluster D; and residues Ser125 and Ile127 from the C-terminal region of the protein. Similar intermediate negative deviations were observed for residues Ser4, Leu6 on

the N-terminal; Arg14, Glu19 in cluster A; Val58–Asn59, Arg63 and Leu65 in cluster B; Glu105 in cluster C; and Ser136 at the C-terminal of the protein.

### 3.4. Insights into inhibition of self-association of GED by I697A mutation

As mentioned earlier, the I697A single point mutation significantly alters the association characteristics of the GED protein [17]. Our results discussed above provide useful insights into this phenomenon. We observed that in the denatured state, where one can observe intrinsic preferences, the mutation at position 82 along the sequence causes structural perturbations at many regions along the sequence and these coincide with the regions showing dynamics perturbations as well. As mentioned above, this may be attributed to transient folding of the chain in the denatured state, as a result of which perturbations at one place can get relayed to other regions of the protein. The mutation, I697A, changes hydrophobicity of the local environment in the protein structure; Ile has a hydropathy index of 4.5 and Ala has an index of 1.8 [34]. Then, by way of transient association of the hydrophobic clusters A, B, C and D along the chain [23] it causes changes in the structural preferences in those regions in the denatured state. The mutation, thus, disturbs the hydrophobic pocket which is required for GED–GED interaction leading to self-assembly in the native state.

It is now a well accepted concept that protein folding starting from an unfolded state initiates according to the structural preferences and local dynamics present in the unfolded state [35]. Since WT GED and I697A have different residual structural components in their denatured state, it can be said with a certain degree of confidence that both also have different structural preferences in their very early stage of protein folding which may take them to acquire a different structure and/or follow different conformational dynamics. Thus, the effect that any mutation may have on the unfolded state may eventually flow towards the folded state. This can indeed influence the self-association property of the protein.

## 4. Conclusions

In conclusion, our results show that the substitution of a hydrophobic residue, isoleucine by another less hydrophobic residue alanine in GED, results in the perturbation of dynamics and the associated topological fluctuations in the denatured state of GED. This causes substantial variations in the structure and dynamics at many remote places along the chain. These would influence early stages of protein folding pathways and eventually the final states where the protein chain may land. Our results provide, on one hand, an understanding of the subtleties of the denatured states, and on the other provide rationales as to how a single point mutation can have dramatic influence on the stability and behavior of proteins with regard to folding, misfolding and association, in general.

## Acknowledgements

We thank the Government of India for providing financial support to the National Facility for High Field NMR at TIFR, India. The authors acknowledge Dr. Rohit Mittal for the GED clone. The help extended by Mr. Bharat T. Kansara and Ms. Mamata Kombrabail are deeply acknowledged. Jeetender Chugh is the recipient of TIFR Alumni Association fellowship for career development though the years 2002–2005.

## References

[1] C. Tanford, Protein denaturation. C. Theoretical models for the mechanism of denaturation, Adv. Protein Chem. 24 (1970) 1–95.
[2] E.S. Rowe, C. Tanford, Equilibrium and kinetics of the denaturation of a homogeneous human immunoglobulin light chain, Biochemistry 12 (1973) 4822–4827.
[3] C.B. Anfinsen, H.A. Scheraga, Experimental and theoretical aspects of protein folding, Adv. Protein Chem. 29 (1975) 205–300.
[4] C.M. Dobson, Experimental investigation of protein folding and misfolding, Methods 34 (2004) 4–14.
[5] T.K. Kumar, C. Yu, Monitoring protein folding at atomic resolution, Acc. Chem. Res. 37 (2004) 929–936.
[6] K. Lindorff-Larsen, P. Rogen, E. Paci, M. Vendruscolo, C.M. Dobson, Protein folding and the organization of the protein topology universe, Trends Biochem. Sci. 30 (2005) 13–19.
[7] K.A. Dill, H.S. Chan, From Levinthal to pathways to funnels, Nat. Struct. Biol. 4 (1997) 10–19.
[8] C.M. Dobson, M. Karplus, The fundamentals of protein folding: bringing together theory and experiment, Curr. Opin. Struct. Biol. 9 (1999) 92–101.
[9] H.J. Dyson, P.E. Wright, Elucidation of the protein folding landscape by NMR, Methods Enzymol. 394 (2005) 299–321.
[10] C.P. van Mierlo, J.M. van den Oever, E. Steensma, Apoflavodoxin (un)folding followed at the residue level by NMR, Protein Sci. 9 (2000) 145–157.
[11] C.P. van Mierlo, E. Steensma, Protein folding and stability investigated by fluorescence, circular dichroism (CD), and nuclear magnetic resonance (NMR) spectroscopy: the flavodoxin story, J. Biotechnol. 79 (2000) 281–298.
[12] C.A. Royer, Fluorescence spectroscopy, Methods Mol. Biol. 40 (1995) 65–89.
[13] C.N. Pace, Determination and analysis of urea and guanidine hydrochloride denaturation curves, Methods Enzymol. 131 (1986) 266–280.
[14] J.E. Hinshaw, S.L. Schmid, Dynamin self-assembles into rings suggesting a mechanism for coated vesicle budding, Nature 374 (1995) 190–192.
[15] J.E. Hinshaw, Dynamin and its role in membrane fission, Annu. Rev. Cell Dev. Biol. 16 (2000) 483–519.
[16] B.D. Song, D. Yarar, S.L. Schmid, An assembly-incompetent mutant establishes a requirement for dynamin self-assembly in clathrin-mediated endocytosis in vivo, Mol. Biol. Cell 15 (2004) 2243–2252.
[17] J. Chugh, A. Chatterjee, A. Kumar, R.K. Mishra, R. Mittal, R.V. Hosur, Structural characterization of the large soluble oligomers of the GTPase effector domain of dynamin, FEBS J. 273 (2006) 388–397.
[18] M.F. Richter, M. Schwemmle, C. Herrmann, A. Wittinghofer, P. Staeheli, Interferon-induced MxA protein. GTP binding and GTP hydrolysis properties, J. Biol. Chem. 270 (1995) 13512–13517.
[19] M.A. Accola, B. Huang, M.A. Al, M.A. McNiven, The antiviral dynamin family member, MxA, tubulates lipids and localizes to the smooth endoplasmic reticulum, J. Biol. Chem. 277 (2002) 21829–21835.
[20] C. Janzen, G. Kochs, O. Haller, A monomeric GTPase-negative MxA mutant with antiviral activity, J. Virol. 74 (2000) 8202–8206.
[21] S. Schwarzinger, P.E. Wright, H.J. Dyson, Molecular hinges in protein folding: the urea-denatured state of apomyoglobin, Biochemistry 41 (2002) 12681–12686.
[22] J. Chugh, S. Sharma, R.V. Hosur, NMR insights into a megadalton-sized protein self-assembly, Protein Sci. in press, doi:10.1110/ps.035840.108.
[23] J. Chugh, S. Sharma, R.V. Hosur, Pockets of short-range transient order and restricted topological heterogeneity in the guanidine-denatured state ensemble of GED of dynamin, Biochemistry 46 (2007) 11819–11832.
[24] R. Murugan, S. Mazumdar, Role of substrate on the conformational stability of the heme active site of cytochrome P450cam: effect of temperature and low concentrations of denaturants, J. Biol. Inorg. Chem. 9 (2004) 477–488.
[25] S. Patel, A.F. Chaffotte, F. Goubard, E. Pauthe, Urea-induced sequential unfolding of fibronectin: a fluorescence spectroscopy and circular dichroism study, Biochemistry 43 (2004) 1724–1735.
[26] N.A. Farrow, R. Muhandiram, A.U. Singer, S.M. Pascal, C.M. Kay, G. Gish, S.E. Shoelson, T. Pawson, J.D. Forman-Kay, L.E. Kay, Backbone dynamics of a free and phosphopeptide-complexed Src homology 2 domain studied by 15N NMR relaxation, Biochemistry 33 (1994) 5984–6003.
[27] P.L. Privalov, N.N. Khechinashvili, A thermodynamic approach to the problem of stabilization of globular protein structure: a calorimetric study, J. Mol. Biol. 86 (1974) 665–684.
[28] P.L. Privalov, Stability of proteins: small globular proteins, Adv. Protein Chem. 33 (1979) 167–241.
[29] F. Rashid, S. Sharma, B. Bano, Comparison of guanidine hydrochloride (GdnHCl) and urea denaturation on inactivation and unfolding of human placental cystatin (HPC), Protein J. 24 (2005) 283–292.
[30] J.K. Kamal, M. Nazeerunnisa, D.V. Behere, Thermal unfolding of soybean peroxidase. Appropriate high denaturant concentrations induce cooperativity allowing the correct measurement of thermodynamic parameters, J. Biol. Chem. 277 (2002) 40717–40721.
[31] J.K. Kamal, D.V. Behere, Thermal and conformational stability of seed coat soybean peroxidase, Biochemistry 41 (2002) 9034–9042.
[32] H.S. Pappa, A.E. Cass, A step towards understanding the folding mechanism of horseradish peroxidase. Tryptophan fluorescence and circular dichroism equilibrium studies, Eur. J. Biochem. 212 (1993) 227–235.
[33] A. Chatterjee, P. Mridula, R.K. Mishra, R. Mittal, R.V. Hosur, Folding regulates autoprocessing of HIV-1 protease precursor, J. Biol. Chem. 280 (2005) 11369–11378.
[34] J. Kyte, R.F. Doolittle, A simple method for displaying the hydropathic character of a protein, J. Mol. Biol. 157 (1982) 105–132.
[35] H.J. Dyson, P.E. Wright, Unfolded proteins and protein folding studied by NMR, Chem. Rev. 104 (2004) 3607–3622.